Infrared contrast of crude-oil-covered water surfaces

Wei-Chuan Shih* and A. Ballard Andrews

Schlumberger-Doll Research, 1 Hampshire Street, Cambridge, Massachusetts 02139, USA
**Corresponding author: wshih@alum.mit.edu*

Received September 8, 2008; accepted October 18, 2008;
posted November 17, 2008 (Doc. ID 101247); published December 12, 2008

Infrared oil spill detection utilizes either temperature or emissivity contrast of native and oil-covered water surfaces. In particular, the thickness dependent radiance contrast due to thin film interference has been studied. Together with detection boundaries derived from the radiative transfer equation, we can explain historically observed daytime contrast reversal and our observations during nighttime, better contrast from thin oil slicks than from thick films, which to our knowledge has not been mentioned in the literature. These findings have important implications to long-wavelength infrared (LWIR) instrument design and data interpretation for crude oil spill detection. © 2008 Optical Society of America

OCIS codes: 260.3060, 260.3160, 280.6780.

Remote sensing of crude oil spills on sea surfaces is of great importance for protecting the environment and managing disasters. Passive optical imaging has been widely employed in environmental monitoring in part because the sensors are less complex and lower in cost, but also because a large target area can be rapidly scanned and processed. In our development of an oil spill detection system, thermal imaging in the long-wavelength infrared [(LWIR), 8–14 μm] has been incorporated into a multiband detection system. LWIR imaging of environmental scenes has two distinct advantages over imaging in other optical wavelength bands. (1) Since the solar spectrum peaks in the visible (~500 nm), LWIR measurements are much less sensitive to solar radiation compared to shorter wavelength bands. (2) Thermal emission of objects at a common ambient temperature (~300 K) peaks in the LWIR band. Therefore LWIR imaging enjoys superior signal strength compared to other IR wavelength bands such as mid-wavelength infrared (3–5 μm).

LWIR remote sensing has been utilized for oil spill detection in the past [1–4]. Positive contrast occurs when the oil covered water surface appears brighter than the native water surface, and negative contrast results when it appears darker. Owing to solar differential heating, oil films on water can reach a higher temperature on sunny days ($T_{\text{oil}} > T_{\text{water}}$); this temperature difference is the dominant contrast mechanism for daytime oil spill detection. However when there is little differential heating, e.g., on a cloudy day or at nighttime, the bulk emissivity difference between crude oil and water ($\varepsilon_{\text{oil}} < \varepsilon_{\text{water}}$) has been identified as a complementary contrast mechanism for detection. Because artificial illumination is not needed, LWIR imaging is a unique modality for nighttime passive optical remote sensing.

In several studies of crude oil spillage, researchers observed that the apparent daytime contrast of native and oil-covered sea surfaces depends on the thickness of the oil film [1–3]. It has also been observed that contrast reversal, from positive to negative, occurs when the oil film becomes thinner. The transition thickness between positive and negative contrast was known to occur between 50 and 150 μm. A plausible explanation for this is that since the oil film is thin, it is essentially in thermal equilibrium with the water underneath, and thus the oil appears cooler because of its intrinsically lower bulk emissivity. However, this explanation does not account for heavier crude oils (which have a higher absorption coefficient) and ignores the possibility that other physical phenomena can play a role. Recently, we developed an analytical model based on the radiative transfer theory and interference effects to provide an alternative explanation for this phenomenon [5]. In this Letter, we consider the remote sensing radiative transfer equation and delineate detection boundaries with respect to crude oil optical properties and detector sensitivity. Based on the model, we calculate the radiance contrast for cases with and without differential heating. Further, we present the first experimental evidence to demonstrate the role thickness dependent radiance contrast plays in nighttime detection of oil spills.

In LWIR remote sensing, total radiance collected by a detector has four possible components [6]: (a) emission from substances within the line of sight of the detector, (b) surface emission, (c) direct solar reflection, and (d) reflected sky radiance. Terms (a) and (c) can be neglected for short-range applications without the sun in the scene. Thus, the radiance difference (ΔL) between oil-covered and native water surfaces can be described as $\Delta L = \Delta\varepsilon_{\text{oil/water–water}}\ \Delta B_{\text{water–sky}} + \varepsilon_{\text{oil/water}}\ \Delta B_{\text{oil/water–water}}$ [Eq. (1)], where $\Delta\varepsilon_{\text{oil/water–water}}$ is the emissivity difference between the oil-covered and the native water surfaces, $\Delta B_{\text{water–sky}}$ is the blackbody radiation difference between the native water surface and the sky, $\varepsilon_{\text{oil/water}}$ is the emissivity of the oil-covered water surface, and $\Delta B_{\text{oil/water–water}}$ is the blackbody radiation difference between the oil-covered and the native water surfaces. Note that Eq. (1) is applicable to a monochromatic as well as a polychromatic case as long as proper integration is carried out over the wavelength. Using the differences in blackbody radiation as inde-

0146-9592/08/243019-3/$15.00

pendent variables, detection boundaries are delineated in Fig. 1(a) by two parallel lines with intercepts at $(X,Y)=(\delta B/\Delta\varepsilon_{\text{oil/water–water}}, \delta B/\varepsilon_{\text{oil/water}})$, where δB is the noise equivalent radiance difference of the detector. Positive contrast is observed in the region above the upper detection boundary, negative contrast is observed in the region below the lower detection boundary, and the region in between represents a range of contrast that is outside the sensitivity range of the detector. Note that for current commercial microbolometers with thermal sensitivity ~80 mK at 293 K, the intercepts are (X,Y) ~$(314,6.51)$ (μW cm^{-2} str^{-1}) for detection of a typical optically thick crude oil film. In addition, since $X \gg Y$, the detection boundaries are much further out on the X axis than shown in Fig. 1(a), where the scale has been exaggerated for illustration.

A plausible explanation for the historically observed thickness dependent daytime contrast reversal can be identified using points A and B in Fig. 1(a). At a fixed $\Delta B_{\text{water–sky}} > X$, if the differential heating effects diminish as the oil film becomes thinner, which is likely because there is less absorbing liquid, contrast reversal can occur as it moves from A to B. However, this explanation does not account for that a thin layer of heavy crude oil can absorb significantly. As indicated in our previous paper, $\Delta\varepsilon_{\text{oil/water–water}}$ is oil film thickness dependent; it becomes more negative when the oil film becomes thinner than a certain transition thickness. To provide an alternative explanation to this phenomenon, we have developed an analytical model based on the radiative transfer theory and interference effects [5].

Figure 1(b) displays the emissivity of the oil-covered and the native water surfaces for three different oil film thicknesses. It is observed that the frequency of the sinusoidal emissivity fluctuation increases as the oil film thickness increases. If the entire range of 8–14 μm is considered as a single band, the average emissivity also increases as the thicknesses increases. In addition, the LWIR emissivity versus oil film thickness is displayed in Fig. 2(a). It is observed that the emissivity decreases to ~0.93 and then exponentially increases toward the bulk oil emissivity at larger thicknesses. Note that the fluctuation on top of the exponential curve is a result of discrete and finite sampling in the wavelength.

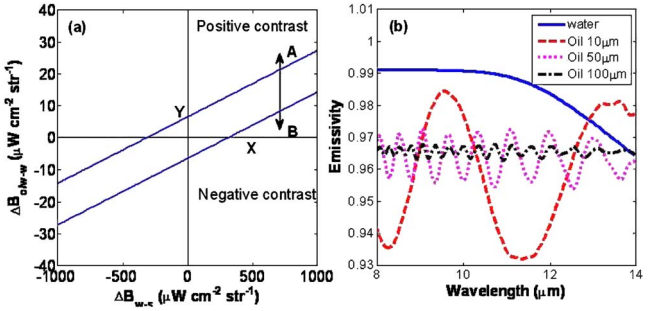

Fig. 1. (Color online) (a) Detection boundaries delineated using Eq. (1). See text for detailed discussion. (b) Emissivity of oil covered and native water surfaces (solid curve). Three oil film thicknesses were simulated: 10 μm (dashed curve), 50 μm (dotted curve), and 100 μm (dashed–dotted curve).

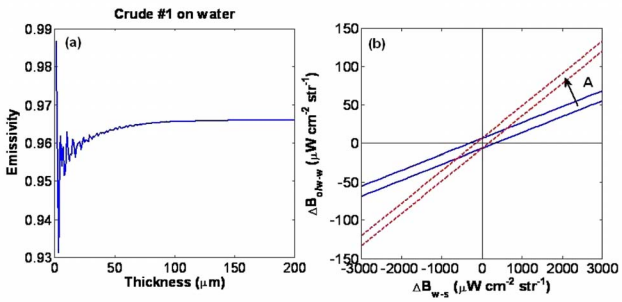

Fig. 2. (Color online) (a) Total emissivity versus the oil film thickness. (b) Detection boundaries delineated using Eq. (1). See text for detailed discussion.

The thickness dependent emissivity can be used in conjunction with the detection boundaries obtained from Eq. (1) to describe daytime contrast reversal. As shown in Fig. 2(b), when the oil film becomes thinner, the original detection boundaries (solid parallel lines) are rotated counterclockwise to a second set of boundaries (dashed parallel lines), reflecting changes in $\Delta\varepsilon_{\text{oil/water–water}}$ (from −0.02 to −0.03) and $\varepsilon_{\text{oil/water}}$ (from 0.965 to 0.955), and thus the new intercepts $(X',Y')=(157,6.65)$. Under clear sky conditions with $\Delta B_{\text{water–sky}} \sim 3350$ μW cm^{-2} str^{-1} [7], contrast reversal can occur even if there is no change in temperature differences, i.e., both $\Delta B_{\text{water–sky}}$ and $\Delta B_{\text{oil–water}}$ are fixed [e.g., Fig. 2(b), point A], thus providing an explanation entirely based on thickness variations. Note that as $\varepsilon_{\text{oil/water}} \gg \Delta\varepsilon_{\text{oil/water–water}}$, the change of the x intercept ($|\Delta X|$) is much larger than that of the y intercept ($|\Delta Y|$).

We discuss here two important observations that may lead to novel detection mechanisms. (1) With an integrated band from 8 to 14 μm, a spatially nonuniform oil film thickness can lead to radiance variations, which is less likely to occur from a clean water surface unless there is large spatial temperature variations on the surface. (2) The sinusoidal fluctuation in emissivity [Fig. 1(b)] can be measured by a multichannel instrument, such as a spectrometer, whereas a flat (8–10 μm) and monotonically decreasing trend (10–14 μm) is obtained from a clean water surface. These two new contrast mechanisms will be explored in the future.

Under clear sky conditions, normalized radiance contrasts are calculated for the cases with and without differential heating with results displayed in Figs. 3(a) and 3(b), respectively. The normalized radiance contrast used here is defined as $C=\Delta L/L_{\text{water}}$. In Fig. 3(a), where the oil temperature is 2 K higher than the water temperature, it is observed that contrast reversal occurs around 50 μm. Note that the exact transition thickness depends on a crude oil type and observation angle [5]. In addition, all simulations were performed for normal incidence in this Letter. In Fig. 3(b), the contrast is always negative without differential heating, as expected. However, the thinner oil film is associated with better contrast (more negative) than thicker ones. To our knowledge,

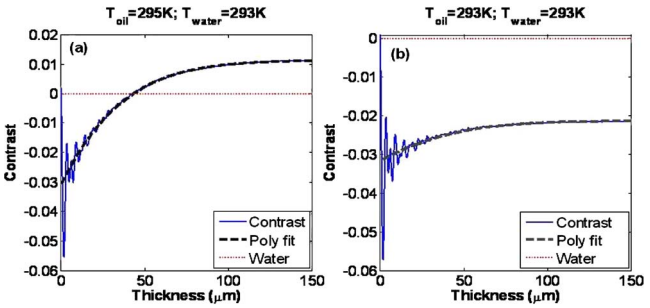

Fig. 3. (Color online) (a) Radiance contrast versus oil film thickness with differential heating T_{oil}, 295 K; T_{water}, 293 K. (b) Radiance contrast versus oil film thickness without differential heating T_{oil}, 293 K; T_{water}, 293 K. In both (a) and (b), the dotted lines represent no contrast as compared to the clean water surface. The solid curves represent the calculated contrast, and the dashed curves are polynomial fits to the solid curves for visual guidance.

the observation that thinner oil films appear to possess better contrast than thicker films has not been previously mentioned in the literature. Note that a 1% difference in contrast corresponds to ~0.5°C (at ~293 K) and therefore can be readily detected by a microbolometer-based camera.

We performed an outdoor nighttime experiment to investigate thickness dependent radiance contrast without differential heating under clear sky conditions. The experiment was carried out at Ohmsett, the National Oil Spill Research Facility in Leonardo, N.J. The ambient air and water temperatures were ~48.2°F and ~52.5°F, respectively. Crude oil (Endicott, American Petroleum Institute gravity 23) was released into five target cells made of polyvinyl chloride pipes floating in a 17 m × 200 m tank filled with sea water. An LWIR camera (Thermal-Eye 4500AS, L3 Communications) and a visible camera with flashlight (PowerShot SD400, Canon) were used with an observation angle ~15° from nadir. Equal amounts of oil (~100 mL) were released into cells 4–6, while much less in cells 1–2, on the order of ~1 mL. Cell 3 was left blank as the control cell. All oil aliquots were from the same container with temperature closed to the ambient air. The images were taken 10 min after all oil was dispensed, allowing enough time for temperature stabilization. The visible image is displayed in Fig. 4(a), showing that the large quantity releases in cells 4–6 are apparent but not the small quantity releases in cells 1 and 2. However, significantly better contrast (more negative) is observed from cells 1 and 2 in Fig. 4(b) from the LWIR camera. Average pixel intensity counts were obtained from 11 different localized areas indicated by A to K (see Fig. 4 caption). The contrasts are much better in cells 1 and 2 than those in cells 4–6, thus demonstrating that the contrast is more negative for thinner oil films than

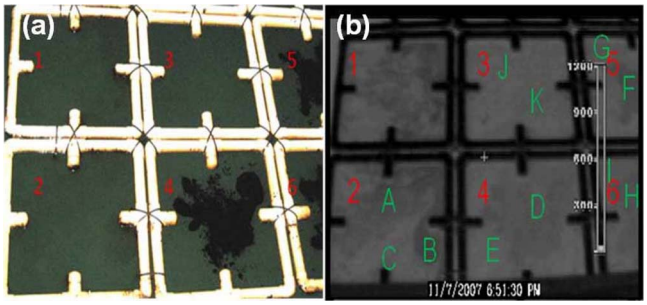

Fig. 4. (Color online) (a) Visible image (with flashlight) taken from ~3.3 m away from the targets during nighttime. (b) LWIR image taken from ~3.3 m away from the targets during nighttime. The average pixel intensity is obtained: (A,B,C)=(68.8,63.7,89.6); (D,E)=(81,91.2); (F,G)=(72,82.7); (H,I)=(80.8,87.2), and (J,K)=(84.2,87.7).

thick ones. This finding has profound implications for nighttime detection of oil spills (or in the absence of differential heating); thin oil slicks can be detected more easily than thick oil films.

In summary, we have presented a thickness dependent infrared radiance contrast model for native and crude-oil-covered water surfaces. This model is based on the radiative transfer theory and the thin film interference effect. Using this model, together with a detection boundary analysis, we can provide an alternative explanation for the historical observations of daytime contrast reversal. Such an explanation is entirely based on thickness variations. Further, the model predicts that thinner oil slicks have better (more negative) contrast than thick films, which has been experimentally verified. Such results suggest that thin oil slicks can be easier to detect in the LWIR than thicker films, especially when differential heating is not effective. Such findings have important implications to oil spill detection regarding fundamental detection and contrast mechanisms.

References

1. R. H. Goodman, *The Remote Sensing of Oil Slicks*, A. E. Lodge, ed. (Wiley, 1989), p. 39.
2. U. Hua, in *Proceedings of IEEE International Geoscience and Remote Sensing Symposium* (IEEE, 1991), p. 1315.
3. R. Horvath, *Optical Remote Sensing of Oil Slicks: Signature Analysis and Systems Evaluation* (University of Michigan, 1971).
4. J. W. Salisbury, D. M. D'Aria, and F. F. Sabins, Remote Sens. Environ. **45**, 225 (1993).
5. W.-C. Shih and A. B. Andrews, Opt. Express **16**, 10535 (2008).
6. C. R. Zeisse, C. P. McGrath, K. M. Littfin, and H. G. Hughes, J. Opt. Soc. Am. A **16**, 1439 (1999).
7. E. E. Bell, L. Eisner, J. Young, and R. A. Oetjen, J. Opt. Soc. Am. **50**, 1313 (1960).